

## Energy Dependence of Particle Multiplicities in Central Au + Au Collisions

B. B. Back,<sup>1</sup> M. D. Baker,<sup>2</sup> D. S. Barton,<sup>2</sup> R. R. Betts,<sup>6</sup> R. Bindel,<sup>7</sup> A. Budzanowski,<sup>3</sup> W. Busza,<sup>4</sup> A. Carroll,<sup>2</sup> J. Corbo,<sup>2</sup> M. P. Decowski,<sup>4</sup> E. Garcia,<sup>6</sup> N. George,<sup>1</sup> K. Gulbrandsen,<sup>4</sup> S. Gushue,<sup>2</sup> C. Halliwell,<sup>6</sup> J. Hamblen,<sup>8</sup> C. Henderson,<sup>4</sup> D. Hicks,<sup>2</sup> D. Hofman,<sup>6</sup> R. S. Hollis,<sup>6</sup> R. Hołyński,<sup>3</sup> B. Holzman,<sup>2</sup> A. Iordanova,<sup>6</sup> E. Johnson,<sup>8</sup> J. Kane,<sup>4</sup> J. Katzy,<sup>4,6</sup> N. Khan,<sup>8</sup> W. Kucewicz,<sup>6</sup> P. Kulinich,<sup>4</sup> C. M. Kuo,<sup>5</sup> W. T. Lin,<sup>5</sup> S. Manly,<sup>8</sup> D. McLeod,<sup>6</sup> J. Michałowski,<sup>3</sup> A. Mignerey,<sup>7</sup> J. Mülmenstädt,<sup>4</sup> R. Nouicer,<sup>6</sup> A. Olszewski,<sup>3</sup> R. Pak,<sup>2</sup> I. C. Park,<sup>8</sup> H. Pernegger,<sup>4</sup> M. Rafelski,<sup>2</sup> M. Rbeiz,<sup>4</sup> C. Reed,<sup>4</sup> L. P. Remsberg,<sup>2</sup> M. Reuter,<sup>6</sup> C. Roland,<sup>4</sup> G. Roland,<sup>4</sup> L. Rosenberg,<sup>4</sup> J. Sagerer,<sup>6</sup> P. Sarin,<sup>4</sup> P. Sawicki,<sup>3</sup> W. Skulski,<sup>8</sup> S. G. Steadman,<sup>4</sup> P. Steinberg,<sup>2</sup> G. S. F. Stephans,<sup>4</sup> M. Stodulski,<sup>3</sup> A. Sukhanov,<sup>2</sup> J.-L. Tang,<sup>5</sup> R. Teng,<sup>8</sup> A. Trzupek,<sup>3</sup> C. Vale,<sup>4</sup> G. J. van Nieuwenhuizen,<sup>4</sup> R. Verrier,<sup>4</sup> B. Wadsworth,<sup>4</sup> F. L. H. Wolfs,<sup>8</sup> B. Wosiek,<sup>3</sup> K. Woźniak,<sup>2,3</sup> A. H. Wuosmaa,<sup>1</sup> and B. Wysłouch<sup>4</sup>

(PHOBOS Collaboration)

<sup>1</sup>*Physics Division, Argonne National Laboratory, Argonne, Illinois 60439-4843*

<sup>2</sup>*Chemistry and C-A Departments, Brookhaven National Laboratory, Upton, New York 11973-5000*

<sup>3</sup>*Institute of Nuclear Physics, Kraków, Poland*

<sup>4</sup>*Laboratory for Nuclear Science, Massachusetts Institute of Technology, Cambridge, Massachusetts 02139-4307*

<sup>5</sup>*Department of Physics, National Central University, Chung-Li, Taiwan*

<sup>6</sup>*Department of Physics, University of Illinois at Chicago, Chicago, Illinois 60607-7059*

<sup>7</sup>*Department of Chemistry, University of Maryland, College Park, Maryland 20742*

<sup>8</sup>*Department of Physics and Astronomy, University of Rochester, Rochester, New York 14627*

(Received 8 August 2001; published 27 December 2001)

We present the first measurement of the pseudorapidity density of primary charged particles in Au + Au collisions at  $\sqrt{s_{NN}} = 200$  GeV. For the 6% most central collisions, we obtain  $dN_{ch}/d\eta|_{|\eta|<1} = 650 \pm 35(\text{sys})$ . Compared to collisions at  $\sqrt{s_{NN}} = 130$  GeV, the highest energy studied previously, an increase by a factor of  $1.14 \pm 0.05$  at 90% confidence level, is found. The energy dependence of the pseudorapidity density is discussed in comparison with data from proton-induced collisions and theoretical predictions.

DOI: 10.1103/PhysRevLett.88.022302

PACS numbers: 25.75.-q

Collisions of gold nuclei at an energy of  $\sqrt{s_{NN}} = 200$  GeV have been studied using the PHOBOS detector. PHOBOS is one of the experiments at the Relativistic Heavy-Ion Collider (RHIC) at Brookhaven National Laboratory aimed at understanding the behavior of strongly interacting matter at high temperature and density. Quantum chromodynamics (QCD), the fundamental theory of strong interactions, predicts that under these conditions, which may be probed in heavy-ion collisions, a new state of matter will be formed, the quark-gluon plasma [1]. In this state, quarks and gluons are no longer confined inside hadrons, as is the case for normal nuclear matter. Information about the particle and energy density achieved in the early stages of the collision process is carried by the pseudorapidity density of particles emitted from the primary collision point [2]. In this analysis, we have determined the pseudorapidity density of charged particles,  $dN_{ch}/d\eta$ , in the most central Au + Au collisions. We focused in particular on the region near  $\eta = 0$ , where  $\eta = -\ln \tan(\theta/2)$  and  $\theta$  is the polar angle from the beam axis.

In combination with results from lower energies, these data permit a systematic analysis of particle production mechanisms in nucleus-nucleus collisions. Extension of the energy range to  $\sqrt{s_{NN}} = 200$  GeV allows a study of the relative contributions of hard parton-parton scatter-

ing processes, which can be calculated using perturbative QCD, and soft processes, which are treated by phenomenological models that describe the nonperturbative sector of QCD. With increasing collision energy, hard processes are expected to contribute an increasingly larger fraction of particle production near midrapidity compared to soft processes.

For Au + Au collisions at RHIC energies, the yield and momentum distribution of particles produced by hard scattering processes may be modified by “jet quenching,” i.e., the energy loss of high momentum partons in the nuclear medium [3]. This phenomenon has been proposed as a diagnostic tool for characterizing the initial parton density in Au + Au collisions at these energies. Preliminary results indicate that in central Au + Au collisions at  $\sqrt{s_{NN}} = 130$  GeV the particle spectra at large transverse momenta, normalized to  $pp$  collisions, indeed change in comparison with lower collision energies [4].

Early predictions for the charged particle pseudorapidity density varied by more than a factor of 2, as shown in [5]. Data on the primary charged particle density  $dN_{ch}/d\eta|_{|\eta|<1}$  at energies of  $\sqrt{s_{NN}} = 56$  and 130 GeV [6] have been analyzed in a wide variety of theoretical models [7–14]. Generally, most models allowed a reasonable description of the energy dependence of  $dN_{ch}/d\eta|_{|\eta|<1}$

up to  $\sqrt{s_{NN}} = 130$  GeV, with a suitable choice of parameters. For the ratio of particle densities near  $\eta = 0$  at 130 and 200 GeV, most calculations predict an increase between 9% and 20%. An interesting exception is the model of Wang and Gyulassy [7]. When the effects of jet quenching are included in their calculation, they not only predict a suppression of particle spectra at high transverse momenta, but also a change of the energy dependence of  $dN_{ch}/d\eta|_{|\eta|<1}$ , leading to an increase of more than 30% between 130 and 200 GeV when the default parameter set is used. The energy dependence of particle production presented here provides important constraints on this effect.

Details of the PHOBOS experimental setup can be found elsewhere [15,16]. The apparatus, shown schematically in Fig. 1, employs silicon detectors for vertex finding, particle tracking, and multiplicity measurements. This analysis is based on the first 6 layers of the 16 layer two-arm spectrometer (SPEC), the two-layer vertex detector (VTX), the single-layer octagon barrel detector (OCT), and the three single-layer ring detectors (RING) located on either side of the interaction point. The acceptance of SPEC, VTX, and OCT includes  $-1 < \eta < 1$ , covering different regions of azimuth. The combined acceptance of OCT and RING detectors reaches  $\eta = \pm 5.4$ . For the 2001 run period, 137 168 silicon channels were read out, of which less than 2% were nonfunctional.

The detector setup also included two sets of 16 scintillator counters (“paddle counters”) located at  $-3.21$  m (PN) and  $3.21$  m (PP) relative to the nominal interaction point along the beam ( $z$ ) axis. These counters covered pseudorapidities between  $3 < |\eta| < 4.5$  and served as the primary event trigger. In combination with the zero-degree calorimeters at  $z = \pm 18.5$  m, which measured the energy deposited by spectator neutrons, PP and PN were also used for off-line event selection.

Monte Carlo (MC) simulations of the detector performance were based on the HIJING event generator [17]

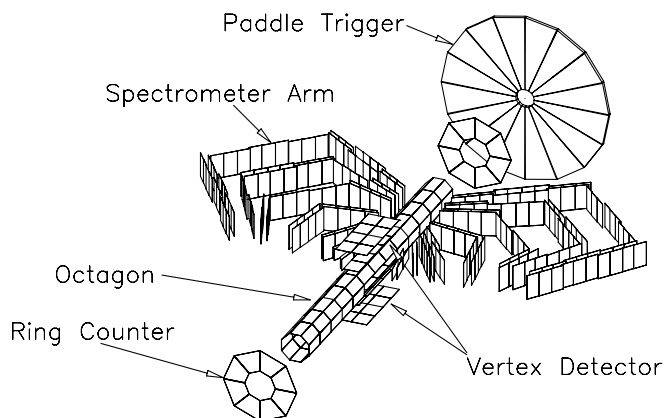


FIG. 1. Active elements of the detector systems used for this analysis. For clarity, one of the paddle counters and the two outer ring counters on each side were omitted and the positions of ring and paddle counters are not to scale.

and the GEANT 3.21 simulation package, folding in the signal response for scintillator counters and silicon detectors. In the calibration of the analysis methods we employed a particle selection procedure that allowed us to iteratively modify the MC output and optimize the agreement of the deposited energy distributions in data and MC.

Details of the trigger performance and the event selection procedure can be found in [6,18]. In the on-line trigger for this data set, we required two or more hits in each paddle counter. Based on MC simulations and trigger studies requiring only a coincidence of one hit in each counter, we estimate that the trigger was sensitive to  $88\% \pm 3\%$  of the total hadronic inelastic cross section. For the selection of central events used here, no contamination from beam-gas or other background collisions was found. We selected the top 6% of the total hadronic cross section with the largest paddle mean, corresponding to the most central collisions with the largest number of participating nucleons. Applying the 6% centrality cut to MC events, we deduce that the average number of participating nucleons in the data is  $\langle N_{part} \rangle = 344 \pm 10(\text{syst})$ .

For the selected central events, the event vertex was determined using the SPEC and VTX subdetectors. Details of the vertex finding procedure can be found in [6,18]. MC studies and correlations between the vertex positions found independently using SPEC and VTX detectors indicate a vertex resolution of better than  $400 \mu\text{m}$  and a vertex finding efficiency of 100% in a fiducial range of  $-10 \text{ cm} < z_{\text{VTX}} < 10 \text{ cm}$ . A total of 639 central events were selected in this vertex range.

The charged particle pseudorapidity density was determined using four independent methods, which have been discussed in detail in previous publications [6,18,19]. We used an analysis of two-hit combinations (tracklets) in SPEC and VTX detectors [6,18], a hit-counting method in OCT and RING [19], and a method based on the observed energy loss in the silicon detectors (“analog method”) [19] for all subdetectors. For all four methods the multiplicity densities  $dN_{ch}/d\eta|_{|\eta|<1}$  were corrected for particles which stop in the material of the beam pipe and the first detector layer, particles from secondary interactions and feed-down products from weak decays of neutral strange particles. The resulting systematic errors on  $dN_{ch}/d\eta|_{|\eta|<1}$  for each method at  $\sqrt{s_{NN}} = 130$  GeV are described in [6,18,19] and range from 4.5% for the SPEC tracklet analysis to 10% for the hit-counting and analog methods. MC studies showed that the systematic uncertainties are essentially the same at  $\sqrt{s_{NN}} = 200$  GeV. The combined result of all four methods is obtained using the inverse square of the estimated uncertainties as weights in the average. Based on MC studies and the comparison of all four independent multiplicity analyses, we estimate the overall systematic uncertainty of the combined result to be less than 6%. The statistical error is negligible.

We obtain a primary charged particle density of  $dN_{ch}/d\eta|_{|\eta|<1} = 650 \pm 35(\text{syst})$  for the 6% most central Au + Au collisions at  $\sqrt{s_{NN}} = 200$  GeV. Normalizing

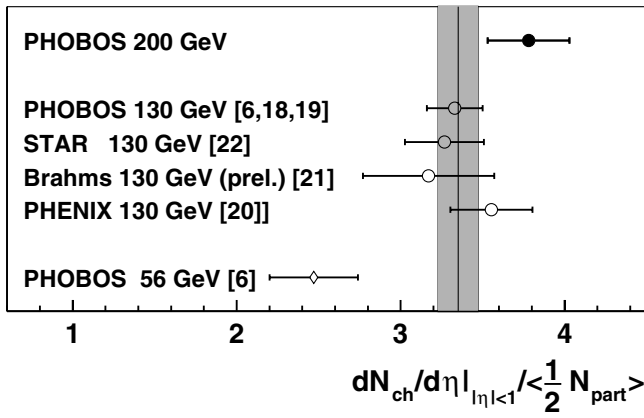


FIG. 2. Summary of RHIC results on the pseudorapidity density near  $\eta = 0$  normalized per participant pair for central Au + Au collisions at  $\sqrt{s_{NN}} = 56, 130,$  and  $200$  GeV. The line and grey area show the averaged result from all four experiments at  $\sqrt{s_{NN}} = 130$  GeV.

per participant pair, we find  $dN_{ch}/d\eta|_{|\eta|<1}/\langle\frac{1}{2}N_{part}\rangle = 3.78 \pm 0.25(\text{syst})$ .

A compilation of all results for  $dN_{ch}/d\eta|_{|\eta|<1}/\langle\frac{1}{2}N_{part}\rangle$  in central Au + Au collisions obtained at RHIC is shown in Fig. 2. It includes results from PHOBOS at  $\sqrt{s_{NN}} = 56$  GeV [6] and from all four RHIC experiments at  $\sqrt{s_{NN}} = 130$  GeV [6,18–22], as well as our new result at  $\sqrt{s_{NN}} = 200$  GeV. For the data from [22] a 1% correction for the different centrality selection was applied, based on the measured centrality dependence from [18,20]. The average value for a 6% centrality selection at 130 GeV is  $dN_{ch}/d\eta|_{|\eta|<1}/\langle\frac{1}{2}N_{part}\rangle = 3.35 \pm 0.12$ , compared to  $3.78 \pm 0.25$  reported here for 200 GeV.

In Fig. 3 the normalized yield per participant is compared to central Au + Au and Pb + Pb collisions at lower energies, including fixed target experiments [23–25]. Also shown for comparison are results from proton-antiproton ( $p\bar{p}$ ) collisions [26] and an interpolation of the  $p\bar{p}$  data. The  $dN_{ch}/d\eta$  values from E866/E917 [23] and NA49 [24,25] were obtained by integrating the measured charged

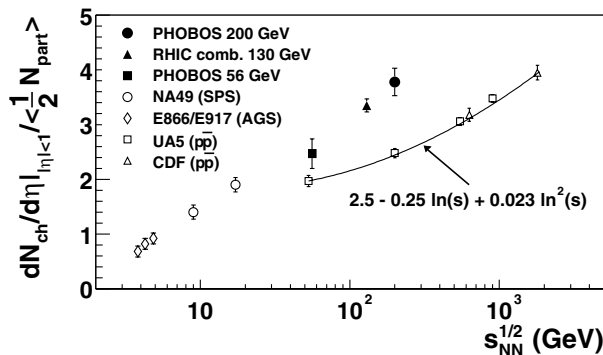


FIG. 3. Energy dependence of the pseudorapidity density normalized per participant pair for central nucleus-nucleus collisions. The data are compared with nucleus-nucleus data from lower energies and  $p\bar{p}$  data [26]. The solid line shows a parametrization of the  $p\bar{p}$  data.

particle rapidity and  $p_T$  distributions. Within the precision of the existing data, an approximately logarithmic rise of  $dN_{ch}/d\eta|_{|\eta|<1}/\langle\frac{1}{2}N_{part}\rangle$  with  $\sqrt{s_{NN}}$  is observed over the full range of collision energies.

A direct measurement of the ratio  $R_{200/130}$  of normalized multiplicity densities  $dN_{ch}/d\eta|_{|\eta|<1}/\langle\frac{1}{2}N_{part}\rangle$  at  $\sqrt{s_{NN}} = 200$  and  $130$  GeV was also performed. The ratio was determined separately for each of the four multiplicity analyses at 130 and 200 GeV and then averaged, weighted with the inverse square of the systematic error for each ratio measurement. Many of the systematic uncertainties in each of the analyses partially cancel, leading to a significant reduction in the uncertainty of the ratio. The theoretical uncertainty in the  $N_{part}$  calculation is also largely eliminated in the ratio. We estimate that the uncertainty from the energy dependence of absorption, feed-down and acceptance corrections is less than 0.03 in  $R_{200/130}$ . Based on MC tests and the comparison of the results for the four different methods, we estimate a total systematic uncertainty of less than 0.05 for the averaged result.

The combined estimate of the ratio of normalized multiplicity densities  $dN_{ch}/d\eta|_{|\eta|<1}/\langle\frac{1}{2}N_{part}\rangle$  at  $\sqrt{s_{NN}} = 200$  and  $130$  GeV, obtained from all four multiplicity analysis methods, is  $R_{200/130} = 1.14 \pm 0.05$ . The quoted uncertainty is entirely systematic and corresponds to a 90% confidence level. In Fig. 4 this value is compared with the  $p\bar{p}$  parametrization [26] and several model calculations. The centrality selection for the models was chosen based on the estimated number of participants in the data. The expected increase from the interpolation of  $p\bar{p}$  results falls slightly below the allowed region. Within the systematic uncertainty, the result is in agreement with most other model predictions. However, we do not observe the large increase expected in the HIJING model [7], which predicted  $R_{200/130} = 1.32$  using the default jet quenching parameters. Further theoretical work will be required to describe both the preliminary results on large  $p_T$  spectra, as well as the energy dependence of particle multiplicities.

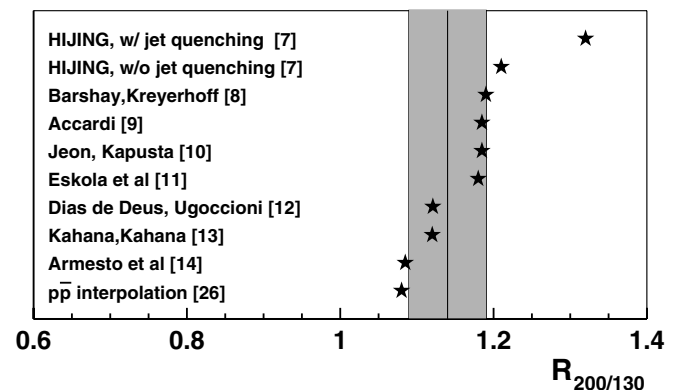


FIG. 4. Ratio  $R_{200/130}$  of pseudorapidity densities  $dN_{ch}/d\eta|_{|\eta|<1}$  at  $\sqrt{s_{NN}} = 200$  and  $130$  GeV. The predicted increase from various models is compared to the observed increase in the data (vertical line). The grey band shows the 90% confidence interval.

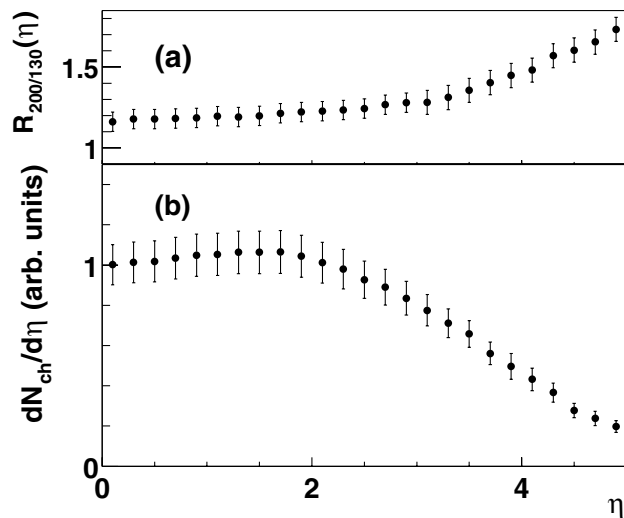


FIG. 5. The lower plot shows the shape of  $dN_{ch}/d\eta$  at  $\sqrt{s_{NN}} = 200$  GeV, obtained from the analog method. On top we show the pseudorapidity dependence of  $R_{200/130}$  using the result of the analog method at both energies. In both plots, the error bars indicate the systematic uncertainty (90% confidence level).

Additional information about the change in particle production from 130 to 200 GeV collision energy can be gained from Figs. 5a and 5b. Using the results from the analog method [19], Fig. 5b shows the shape of the pseudorapidity distribution out to  $\eta = 5$  for central collisions at 200 GeV. The main contributions to the systematic error on  $dN_{ch}/d\eta$  for the analog method are the uncertainties on the energy loss per charged particle and the fraction of background particles. These effects depend on  $\eta$ , leading to the systematic uncertainty in the shape of the pseudorapidity distribution shown by the error bars in Fig. 5b. The statistical error is negligible.

Studies of the signal distributions in data and MC suggest that both the energy loss per particle and the fraction of background particles are very similar at the two energies. This leads to significantly smaller uncertainties in Fig. 5a, which shows the ratio  $R_{200/130}$  as a function of  $\eta$ . A slow rise of the ratio is observed to  $|\eta| \approx 3.5$ , showing a modest increase in particle density between 130 and 200 GeV not only at midrapidity, but over the full central plateau region. Only at large  $\eta$  a steeper rise is seen, corresponding to the widening of the pseudorapidity distribution. This reflects the shift in the fragmentation region due to the larger beam rapidity, which grows from  $y_{beam} = 5.0$  to  $y_{beam} = 5.4$ .

In summary, we report the first measurement of the pseudorapidity density of primary charged particles in Au + Au collisions at  $\sqrt{s_{NN}} = 200$  GeV. Near midrapidity, this density shows an approximately logarithmic evolution over a broad range of collision energies. Going from  $\sqrt{s_{NN}} = 130$  to 200 GeV, the observed increase is a factor of  $1.14 \pm 0.05(\text{syst})$  at 90% confidence level,

corresponding to a moderate increase in initial energy density. Over this energy interval, a smooth evolution of  $dN_{ch}/d\eta$  in all regions of pseudorapidity is seen. These results give further constraints for models including effects of the partonic medium in the early collision stages.

This work was partially supported by U.S. DOE Grants No. DE-AC02-98CH10886, No. DE-FG02-93ER40802, No. DE-FC02-94ER40818, No. DE-FG02-94ER40865, No. DE-FG02-99ER41099, and No. W-31-109-ENG-38, as well as NSF Grants No. 9603486, No. 9722606, and No. 0072204. The Polish groups were partially supported by KBN Grant No. 2 P03B 04916. The NCU group was partially supported by NSC of Taiwan under Contract No. NSC 89-2112-M-008-024.

- [1] See, e.g., J. P. Blaizot, Nucl. Phys. **A661**, 3c (1999).
- [2] J. D. Bjorken, Phys. Rev. D **27**, 140 (1983).
- [3] M. Gyulassy and M. Plümer, Phys. Lett. B **243**, 432 (1990).
- [4] J. Harris *et al.*, in Proceedings of QM 2001 Conference (to be published); W. Zajc *et al.*, in Proceedings of QM 2001 Conference (to be published); K. Adcox *et al.*, nucl-ex/0109003.
- [5] N. Armesto and C. Pajares, Int. J. Mod. Phys. A **15**, 2019 (2000).
- [6] B. B. Back *et al.*, Phys. Rev. Lett. **85**, 3100 (2000).
- [7] X. N. Wang and M. Gyulassy, Phys. Rev. Lett. **86**, 3496 (2001).
- [8] S. Barshay and G. Kreyerhoff, hep-ph/0104303.
- [9] A. Accardi, hep-ph/0104060.
- [10] S. Jeon and J. Kapusta, Phys. Rev. C **63**, 011901 (2001).
- [11] K. J. Eskola *et al.*, hep-ph/0106330.
- [12] J. Dias de Deus and R. Ugoccioni, Phys. Lett. B **491**, 253 (2000).
- [13] D. E. Kahana and S. H. Kahana, Phys. Rev. C **63**, 031901(R) (2001).
- [14] N. Armesto, C. Pajares, and D. Sousa, hep-ph/0104269.
- [15] B. B. Back *et al.*, Nucl. Phys. **A661**, 690 (1999).
- [16] H. Pernegger *et al.*, Nucl. Instrum. Methods Phys. Res., Sect. A **419**, 549 (1998).
- [17] M. Gyulassy and X. N. Wang, Phys. Rev. D **44**, 3501 (1991).
- [18] B. B. Back *et al.*, Phys. Rev. C (to be published).
- [19] B. B. Back *et al.*, Phys. Rev. Lett. **87**, 102303 (2001).
- [20] K. Adcox *et al.*, Phys. Rev. Lett. **86**, 3500 (2001).
- [21] F. Videbaek *et al.*, in Proceedings of QM 2001 Conference (to be published).
- [22] C. Adler *et al.*, Phys. Rev. Lett. **87**, 112303 (2001).
- [23] L. Ahle *et al.*, Phys. Lett. B **476**, 1 (2000); L. Ahle *et al.*, Phys. Lett. B **490**, 53 (2000); B. B. Back *et al.*, Phys. Rev. Lett. **86**, 1970 (2001).
- [24] J. Bächler *et al.*, Nucl. Phys. **A661**, 45 (1999).
- [25] C. Blume *et al.*, in Proceedings of QM 2001 Conference (to be published).
- [26] F. Abe *et al.*, Phys. Rev. D **41**, 2330 (1990).